Probing the cosmic dipole in the radio sky

Using ASKAP for cosmology

Oliver Oayda

PhD Candidate
Sydney Institute for Astronomy
The University of Sydney

Supervised by
Geraint Lewis
Tara Murphy

CSIRO
S&A Colloquium

August 28, 2024

Agenda

Background

The Cosmological Principle

On very large scales, the Universe looks the same everywhere — it is homogeneous and isotropic.

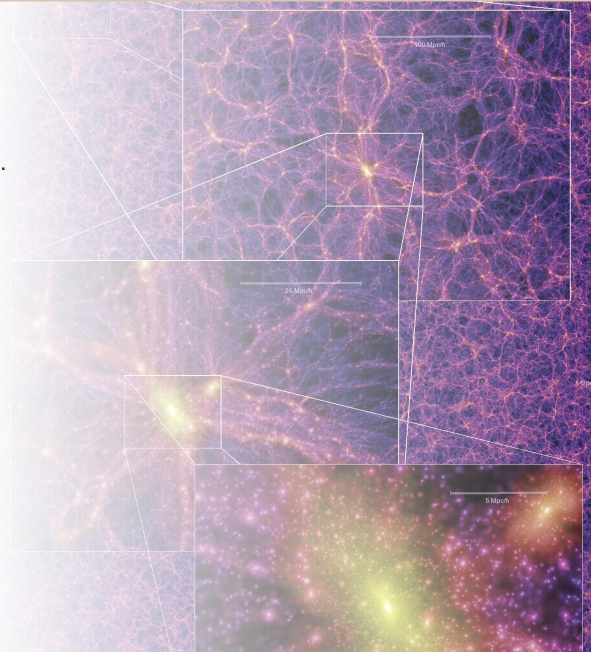

The Cosmological Principle

On very large scales, the Universe looks the same everywhere — it is homogeneous and isotropic.

Foundational assumption in current cosmological framework, e.g. FLRW, Friedmann world models, etc.

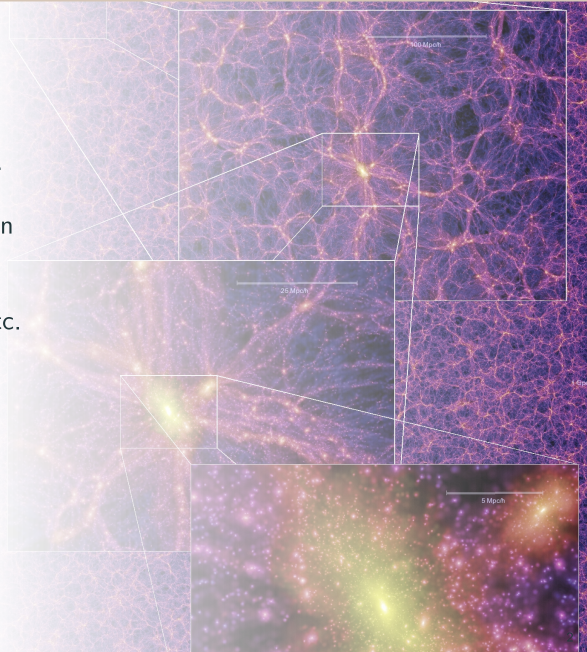

The Cosmological Principle

On very large scales, the Universe looks the same everywhere — it is homogeneous and isotropic.

Foundational assumption in current cosmological framework, e.g. FLRW, Friedmann world models, etc.

$$ds^2 = -c^2 dt^2 + a^2(t)\, d\Sigma^2$$

where

$$d\Sigma^2 = \frac{dr^2}{1 - \kappa r^2} + r^2 d\Omega^2$$

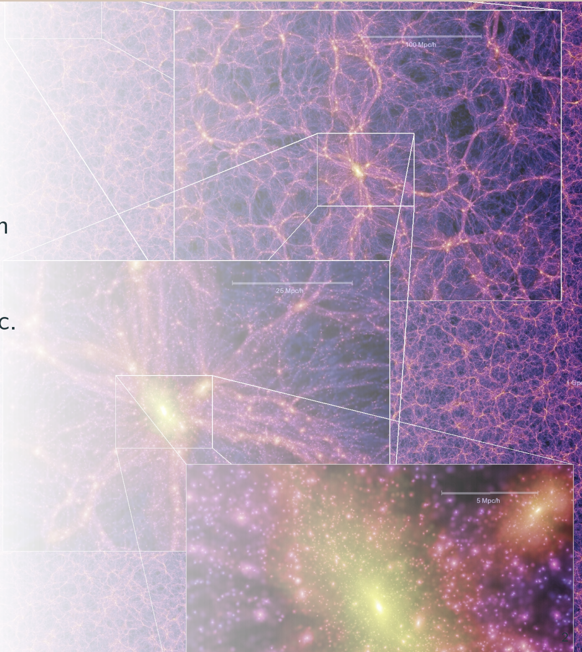

The Cosmic Microwave Background

- The CMB is remarkably smooth ($\Delta T/T \approx 10^{-5}$).

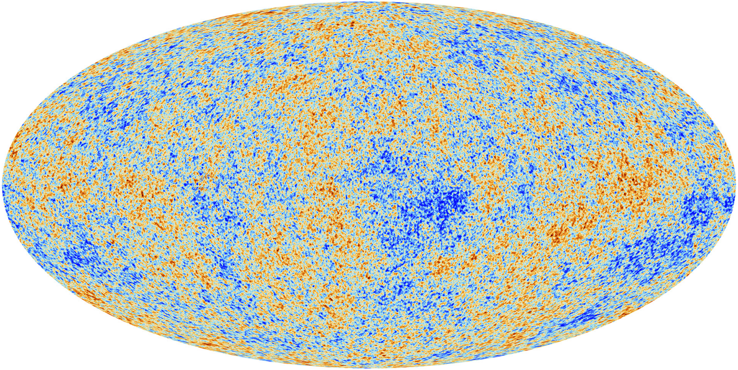

Figure 1: CMB temp. map (dipole subtracted; Planck Collaboration et al., 2020).

The Cosmic Microwave Background

- The CMB is remarkably smooth ($\Delta T/T \approx 10^{-5}$).
- But we see a dipole first ($\Delta T/T \approx 10^{-3}$).

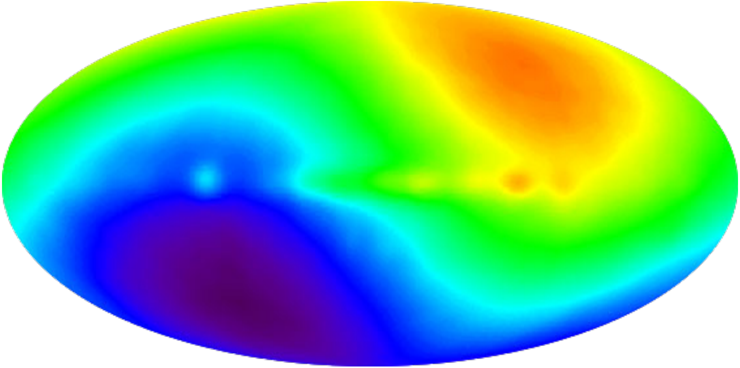

Figure 1: CMB temperature map (dipole included; COBE). ★: dipole direction.

The Cosmic Microwave Background

- The CMB is remarkably smooth ($\Delta T/T \approx 10^{-5}$).
- But we see a dipole first ($\Delta T/T \approx 10^{-3}$).

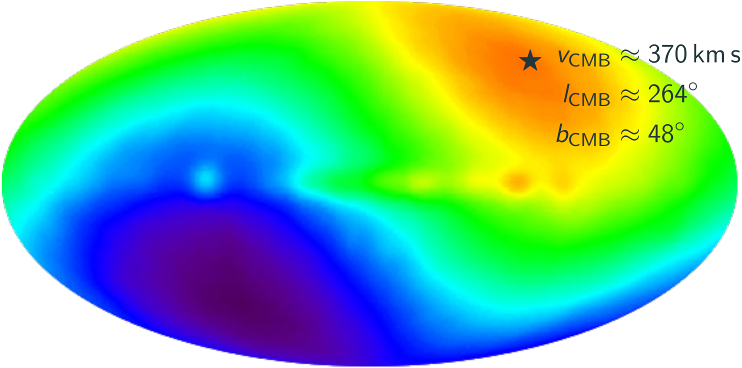

Figure 1: CMB temperature map (dipole included; COBE). ★: dipole direction.

The CMB Dipole

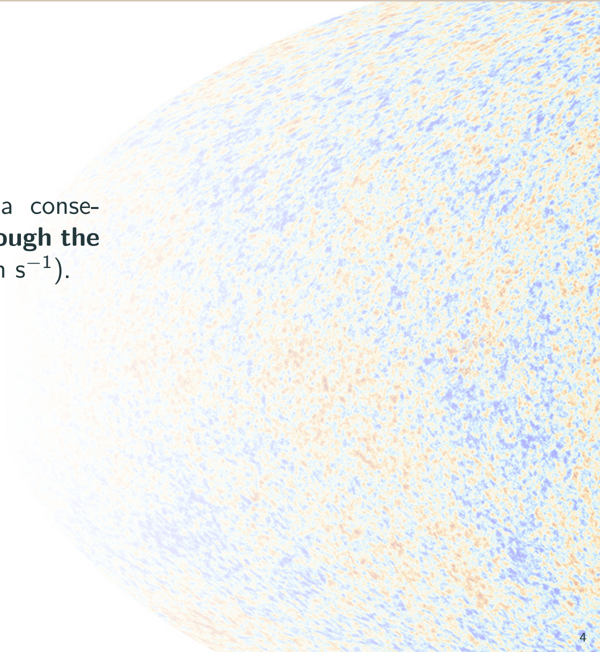

The CMB dipole ★ is a consequence of our **motion through the Universe** ($v_{CMB} \approx 370$ km s^{-1}).

The CMB Dipole

The CMB dipole ★ is a consequence of our **motion through the Universe** ($v_{CMB} \approx 370$ km s^{-1}).

CP → the dipole-removed frame is the frame of cosmic rest.

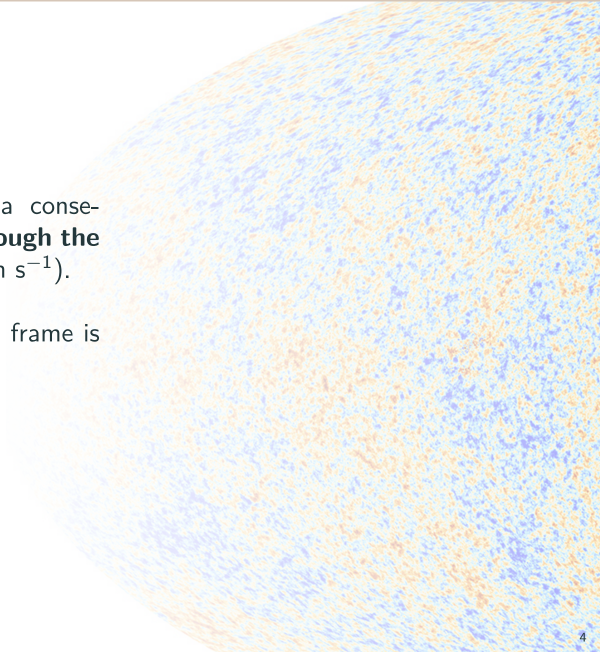

The CMB Dipole

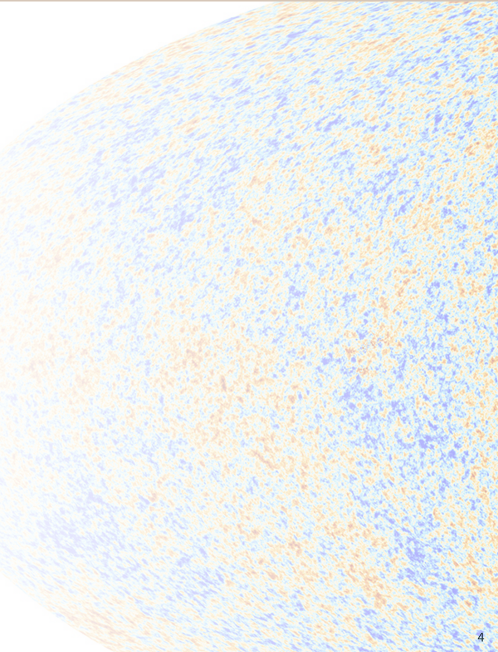

The CMB dipole ★ is a consequence of our **motion through the Universe** ($v_{CMB} \approx 370$ km s^{-1}).

CP → the dipole-removed frame is the frame of cosmic rest.

How do we test the CP?

The Ellis & Baldwin (1984) Test

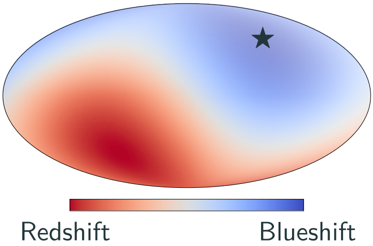

Figure 2: Sketch of the Ellis & Baldwin (1984) test. *Left:* Dipole signal due to Doppler shift. *Right:* Cumulative flux density distribution: number of sources above a given flux density limit S_ν.

The Ellis & Baldwin (1984) Test

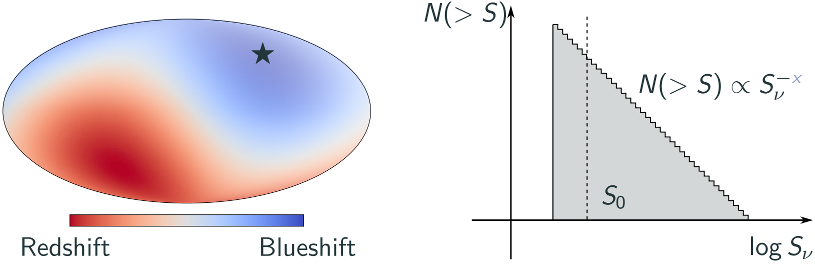

Figure 2: Sketch of the Ellis & Baldwin (1984) test. *Left:* Dipole signal due to Doppler shift. *Right:* Cumulative flux density distribution: number of sources above a given flux density limit S_ν.

The Ellis & Baldwin (1984) Test

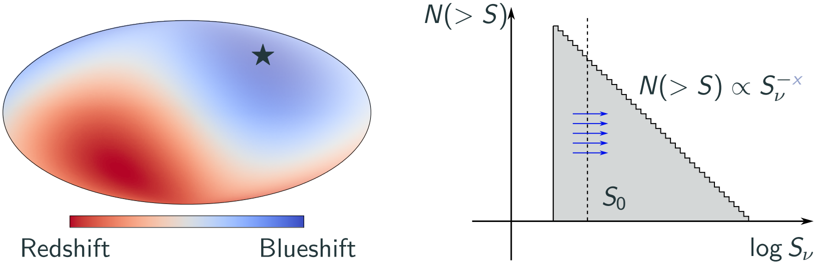

Figure 2: Sketch of the Ellis & Baldwin (1984) test. *Left:* Dipole signal due to Doppler shift. *Right:* Cumulative flux density distribution: number of sources above a given flux density limit S_ν.

The Ellis & Baldwin (1984) Test

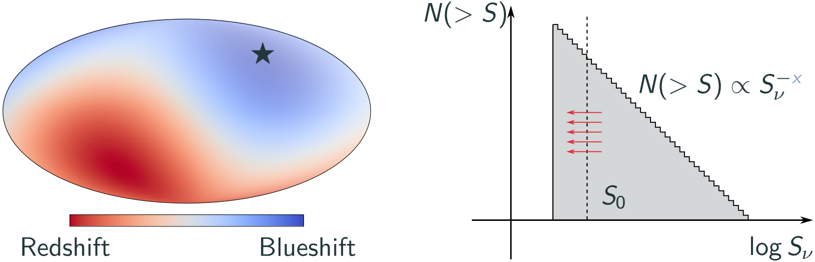

Figure 2: Sketch of the Ellis & Baldwin (1984) test. *Left:* Dipole signal due to Doppler shift. *Right:* Cumulative flux density distribution: number of sources above a given flux density limit S_ν.

The Ellis & Baldwin (1984) Test

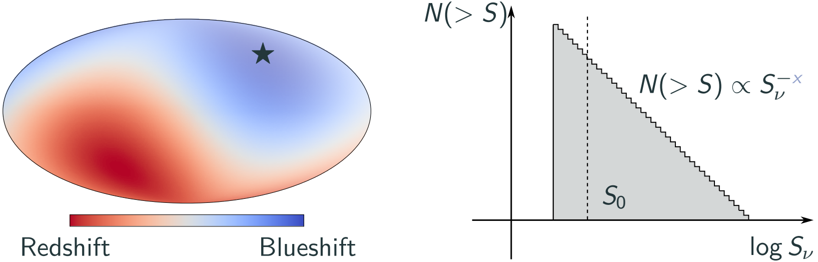

Figure 2: Sketch of the Ellis & Baldwin (1984) test. *Left:* Dipole signal due to Doppler shift. *Right:* Cumulative flux density distribution: number of sources above a given flux density limit S_ν.

The Ellis & Baldwin (1984) Test

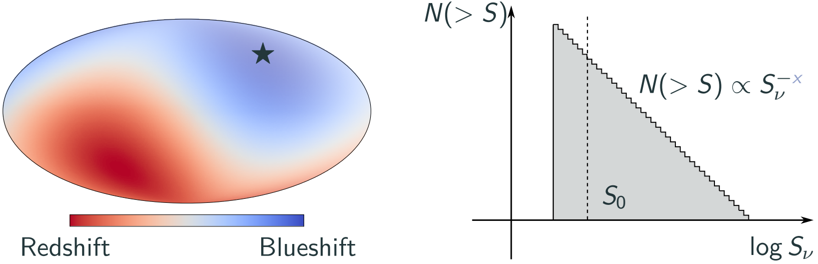

Figure 2: Sketch of the Ellis & Baldwin (1984) test. *Left:* Dipole signal due to Doppler shift. *Right:* Cumulative flux density distribution: number of sources above a given flux density limit S_ν.

We use only **special relativity** to derive how our peculiar motion impacts observables — namely galaxy surveys.

E&B Relation

We use only a handful of relations $\triangleright$ from SR and assumptions $*$ about the source population. Primed variables are our frame.
$\delta = \gamma(1 + \beta \cos \theta)$ and $\beta = v/c$.

E&B Relation

We use only a handful of relations ▷ from SR and assumptions $*$ about the source population. Primed variables are our frame.
$\delta = \gamma(1 + \beta \cos \theta)$ and $\beta = v/c$.

- ▷ We know $\nu' = \nu\delta$ — Doppler shift

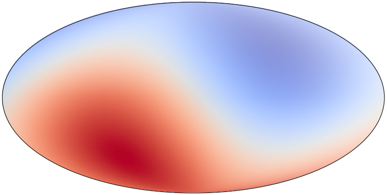

E&B Relation

We use only a handful of relations ▷ from SR and assumptions ∗ about the source population. Primed variables are our frame.
$\delta = \gamma(1 + \beta \cos\theta)$ and $\beta = v/c$.

- ▷ We know $\nu' = \nu\delta$ — Doppler shift
- ∗ We assume that sources follow $S_\nu \propto \nu^{-\alpha}$

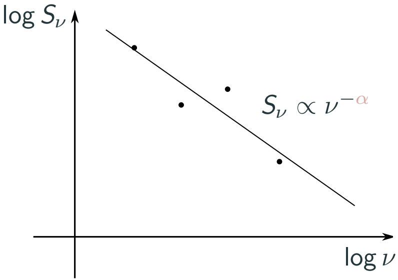

E&B Relation

We use only a handful of relations ▷ from SR and assumptions ∗ about the source population. Primed variables are our frame.
$\delta = \gamma(1 + \beta \cos\theta)$ and $\beta = v/c$.

- ▷ We know $\nu' = \nu\delta$ — Doppler shift
- ∗ We assume that sources follow $S_\nu \propto \nu^{-\alpha}$
- ∗ We assume $N(> S) \propto S_\nu^{-x}$

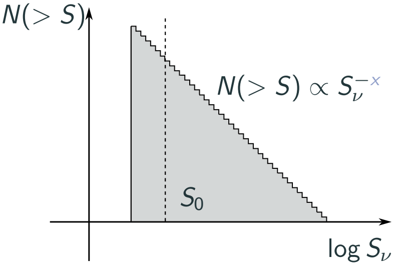

E&B Relation

We use only a handful of relations ▷ from SR and assumptions ∗ about the source population. Primed variables are our frame.
$\delta = \gamma(1 + \beta\cos\theta)$ and $\beta = v/c$.

- ▷ We know $\nu' = \nu\delta$ — Doppler shift
- ∗ We assume that sources follow $S_\nu \propto \nu^{-\alpha}$
- ∗ We assume $N(> S) \propto S_\nu^{-x}$
- ▷ We know $d\Omega' = d\Omega\delta^{-2}$ — relativistic aberration

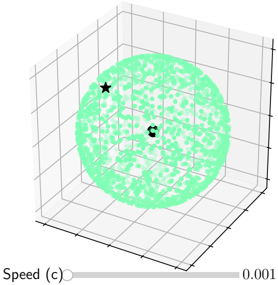

E&B Relation

We use only a handful of relations ▷ from SR and assumptions ∗ about the source population. Primed variables are our frame.
$\delta = \gamma(1 + \beta \cos\theta)$ and $\beta = v/c$.

- ▷ We know $\nu' = \nu\delta$ — Doppler shift
- ∗ We assume that sources follow $S_\nu \propto \nu^{-\alpha}$
- ∗ We assume $N(> S) \propto S_\nu^{-x}$
- ▷ We know $d\Omega' = d\Omega\delta^{-2}$ — relativistic aberration

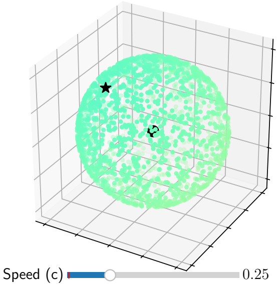

E&B Relation

We use only a handful of relations ▷ from SR and assumptions ∗ about the source population. Primed variables are our frame.
$\delta = \gamma(1 + \beta \cos\theta)$ and $\beta = v/c$.

- ▷ We know $\nu' = \nu\delta$ — Doppler shift
- ∗ We assume that sources follow $S_\nu \propto \nu^{-\alpha}$
- ∗ We assume $N(> S) \propto S_\nu^{-x}$
- ▷ We know $d\Omega' = d\Omega\delta^{-2}$ — relativistic aberration

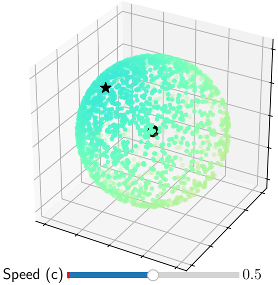

E&B Relation

We use only a handful of relations ▷ from SR and assumptions ∗ about the source population. Primed variables are our frame.
$\delta = \gamma(1 + \beta \cos\theta)$ and $\beta = v/c$.

- ▷ We know $\nu' = \nu\delta$ — Doppler shift
- ∗ We assume that sources follow $S_\nu \propto \nu^{-\alpha}$
- ∗ We assume $N(> S) \propto S_\nu^{-x}$
- ▷ We know $d\Omega' = d\Omega\delta^{-2}$ — relativistic aberration

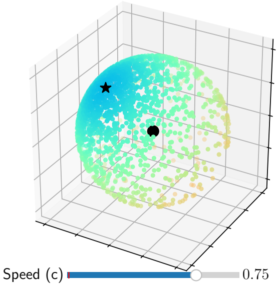

E&B Relation

We use only a handful of relations ▷ from SR and assumptions ∗ about the source population. Primed variables are our frame.
$\delta = \gamma(1 + \beta \cos\theta)$ and $\beta = v/c$.

- ▷ We know $\nu' = \nu\delta$ — Doppler shift
- ∗ We assume that sources follow $S_\nu \propto \nu^{-\alpha}$
- ∗ We assume $N(> S) \propto S_\nu^{-x}$
- ▷ We know $d\Omega' = d\Omega\delta^{-2}$ — relativistic aberration

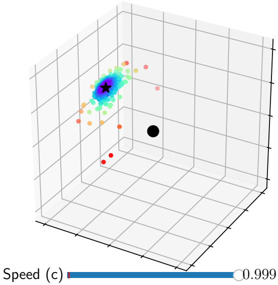

E&B Relation

We use only a handful of relations ▷ from SR and assumptions ∗ about the source population. Primed variables are our frame.
$\delta = \gamma(1 + \beta \cos\theta)$ and $\beta = v/c$.

- ▷ We know $\nu' = \nu\delta$ — Doppler shift
- ∗ We assume that sources follow $S_\nu \propto \nu^{-\alpha}$
- ∗ We assume $N(> S) \propto S_\nu^{-x}$
- ▷ We know $d\Omega' = d\Omega\delta^{-2}$ — relativistic aberration

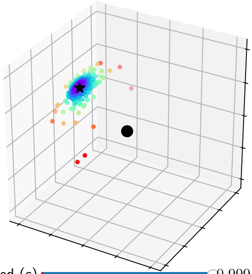

If $dN/d\Omega$ for $S > S_0$ is uniform in the source rest frame, in our frame

$$\left(\frac{dN}{d\Omega}\right)' = \frac{dN}{d\Omega}\,\delta^{2+x(1+\alpha)} \approx \bar{N}(1 + \mathcal{D}\cos\theta).$$

E&B Relation — Dipole Amplitude

The integral source counts above some limiting flux density are then

$$(dN/d\Omega)_{\rm obs} = (dN/d\Omega)_{\rm rest}\,\delta^{2+x(1+\alpha)}.$$

For $(v/c) \ll 1$, $\delta \approx [1+(v/c)\cos\theta]$, so if the sources are isotropic in their own rest frame (as is true in the FRW models) then the observed counts must show a dipole anisotropy over the sky of amplitude $[2+x(1+\alpha)](v/c)$. Thus existence of such an observed anisotropy is a test of the isotropy of the source counts in their rest frame. The great power of this test is that the measurements can be made (and the result must hold) for any source counts, whether in a wide or a narrow solid angle, for flat or steep source spectra, etc, irrespective of selection effects or source evolution, as long as the forward and backward measurements are done in the identical manner.

We find a dipolar modulation in source density $\bar{N}(1+\mathcal{D}\cos\theta)$ where

$$\mathcal{D} = [2 + x(1+\alpha)]\,\beta.$$

E&B Relation — Dipole Amplitude

The integral source counts above some limiting flux density are then

$$(dN/d\Omega)_{\mathrm{obs}} = (dN/d\Omega)_{\mathrm{rest}}\,\delta^{2+x(1+\alpha)}.$$

For $(v/c) \ll 1$, $\delta \approx [1+(v/c)\cos\theta]$, so if the sources are isotropic in their own rest frame (as is true in the FRW models) then the observed counts must show a dipole anisotropy over the sky of amplitude $[2+x(1+\alpha)](v/c)$. Thus existence of such an observed anisotropy is a test of the isotropy of the source counts in their rest frame. The great power of this test is that the measurements can be made (and the result must hold) for any source counts, whether in a wide or a narrow solid angle, for flat or steep source spectra, etc, irrespective of selection effects or source evolution, as long as the forward and backward measurements are done in the identical manner.

We find a dipolar modulation in source density $\bar{N}(1+\mathcal{D}\cos\theta)$ where

$$\boxed{\mathcal{D} = [2 + x(1+\alpha)]\,\beta.}$$

$$\alpha = 0.75,\ x = 1,\ \beta \approx 0.0012 \implies \mathcal{D} = 0.0046.$$

E&B Relation — Dipole Amplitude

The integral source counts above some limiting flux density are then

$$(dN/d\Omega)_{\text{obs}} = (dN/d\Omega)_{\text{rest}}\,\delta^{2+x(1+\alpha)}.$$

For $(v/c) \ll 1$, $\delta \approx [1+(v/c)\cos\theta]$, so if the sources are isotropic in their own rest frame (as is true in the FRW models) then the observed counts must show a dipole anisotropy over the sky of amplitude $[2+x(1+\alpha)](v/c)$. Thus existence of such an observed anisotropy is a test of the isotropy of the source counts in their rest frame. The great power of this test is that the measurements can be made (and the result must hold) for any source counts, whether in a wide or a narrow solid angle, for flat or steep source spectra, etc, irrespective of selection effects or source evolution, as long as the forward and backward measurements are done in the identical manner.

We find a dipolar modulation in source density $\bar{N}(1+\mathcal{D}\cos\theta)$ where

$$\boxed{\mathcal{D} = [2 + x(1+\alpha)]\,\beta.}$$

$$\alpha = 0.75,\ x = 1,\ \beta \approx 0.0012 \implies \mathcal{D} = 0.0046.$$

A 0.5% effect!

Measurements of the Cosmic Dipole

$$\mathcal{D}_{\mathrm{CMB}} = \underbrace{[2 + x(1+\alpha)] \times v_{\mathrm{CMB}}/c}_{\text{expectation}} \quad \text{vs.} \quad \underbrace{N_{\mathrm{cell}} = \bar{N}(1 + \mathcal{D}\cos\theta)}_{\text{reality}}$$

Measurements of the Cosmic Dipole

$$\underbrace{\mathcal{D}_{\mathsf{CMB}} = [2 + x(1+\alpha)] \times v_{\mathsf{CMB}}/c}_{\text{expectation}} \quad \text{vs.} \quad \underbrace{N_{\mathsf{cell}} = \bar{N}(1 + \mathcal{D}\cos\theta)}_{\text{reality}}$$

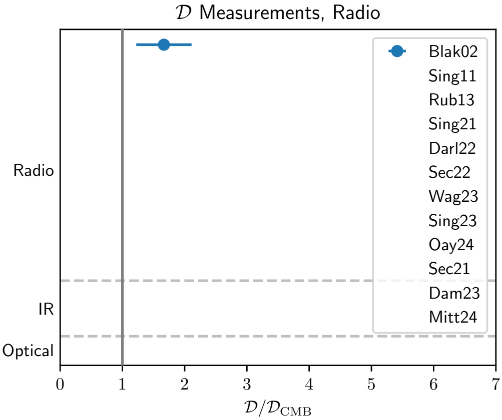

Measurements of the Cosmic Dipole

$$\underbrace{\mathcal{D}_{\text{CMB}} = [2 + x(1+\alpha)] \times v_{\text{CMB}}/c}_{\text{expectation}} \quad \text{vs.} \quad \underbrace{N_{\text{cell}} = \bar{N}(1 + \mathcal{D}\cos\theta)}_{\text{reality}}$$

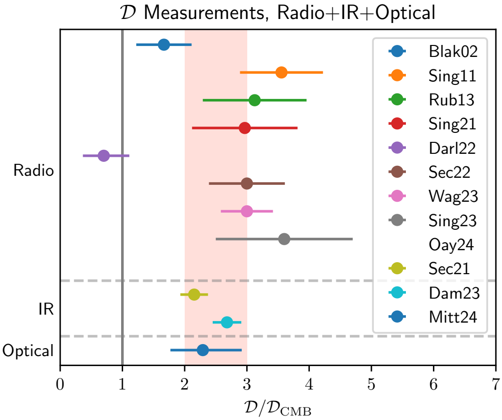

Figure 3: Literature values for $\mathcal{D}$ across radio, optical and near-IR samples (1σ uncertainties). Key samples: **NVSS**, **RACS-low**, **CatWISE2020**, **Quaia**.

Measurements of the Cosmic Dipole

$$\underbrace{\mathcal{D}_{\text{CMB}} = [2 + x(1+\alpha)] \times v_{\text{CMB}}/c}_{\text{expectation}} \quad \text{vs.} \quad \underbrace{N_{\text{cell}} = \bar{N}(1 + \mathcal{D}\cos\theta)}_{\text{reality}}$$

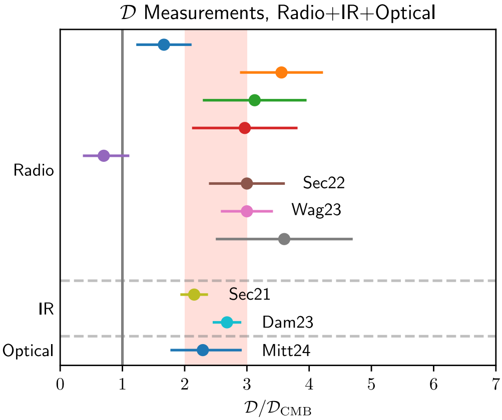

Figure 3: Literature values for $\mathcal{D}$ reported in: Wagenveld et al. (2023); Secrest et al. (2021); Dam et al. (2023); Mittal et al. (2024).

Results of Secrest et al. (2021) — IR

Amplitude $\approx \times 2$ larger than CMB expectation at significance of 5σ.

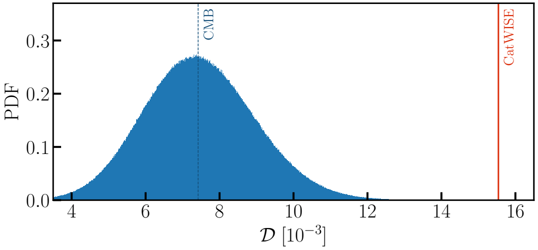

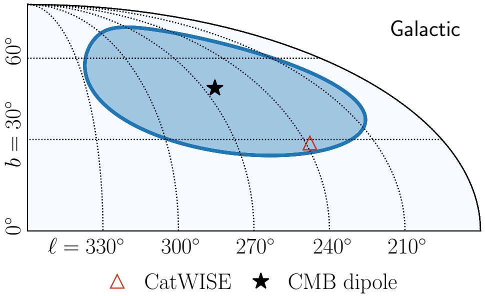

Confirmed by Dam et al. (2023) with a Bayesian approach.

Figure 4: Results from Secrest et al. (2021). *Top:* Statistical significance (5σ) of the CatWISE dipole amplitude. *Bottom*: Significance of the direction of the dipole in CatWISE (2σ contour).

Results of Secrest et al. (2022) — IR + Radio

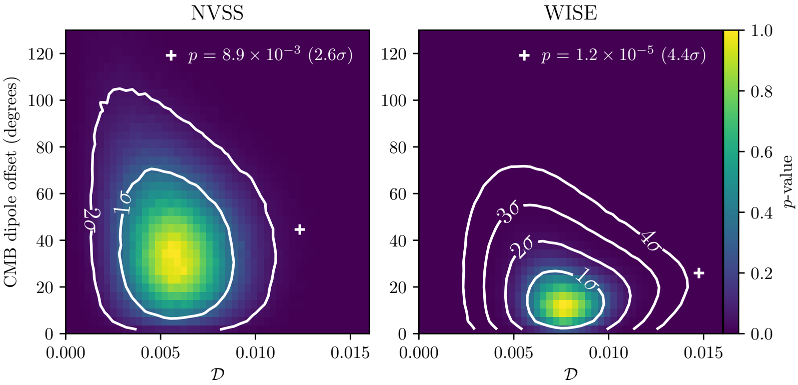

Figure 5: Distribution of dipole amplitudes and offsets for simulated null (CMB) skies as appearing in Secrest et al. (2022). '+' indicates the observed values.

- CatWISE2020 (IR) and NVSS (radio) constructed to be independent.
- Joint significance of 5σ.

Results of Mittal, Oayda & Lewis (2024) — Optical

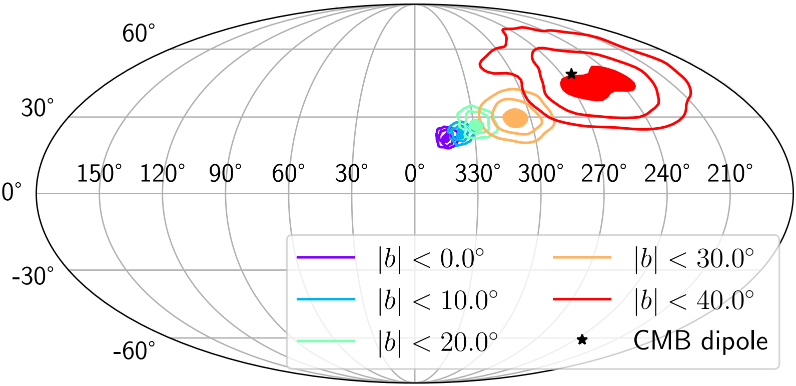

Amplitude $\mathcal{D}$ (10^{-3})	37^{+4}_{-4}	34^{+4}_{-4}	25^{+5}_{-5}	17^{+6}_{-6}	11^{+6}_{-5}	5★

Figure 6: Results from Quaia low ($G < 20.0$) as in Mittal et al. (2024). *Top:* projection of marginal posterior for dipole direction onto the sky. *Bottom:* 2σ credible interval for dipole amplitude by mask choice.

Results of Wagenveld et al. (2023) — Radio

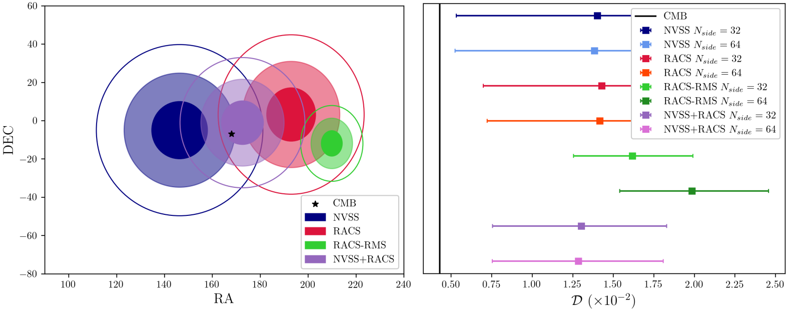

Figure 7: Results of Wagenveld et al. (2023) also point towards an excessive dipole amplitude (but consistent direction).

- '**W23**' — used as prior likelihood later.
- We also analysed NVSS and RACS-low, but with a different approach.

Why is the dipole amplitude larger than expected?

Analysis

Samples We Tested

NVSS (NRAO VLA Sky Survey): 1993–97, 1.4 GHz, northern sky.

RACS-low (Rapid Australian SKA Pathfinder Continuum Survey): 2019–20, 887.5 MHz, southern sky.

Figure 8: *Top:* VLA in New Mexico (credit: NRAO). *Bottom:* Australian SKA Pathfinder in Western Australia (credit: CSIRO).

Some Systematic Effects

Some issues to consider:

Some Systematic Effects

Some issues to consider:

- Catalogue completeness at some S_ν.

Some Systematic Effects

Some issues to consider:

- Catalogue completeness at some S_ν.
- Declination-dependent systematics.

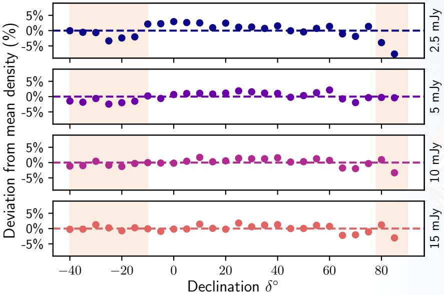

Figure 9: Deviation from mean source density by δ° (NVSS). *Shaded brown:* DnC config.

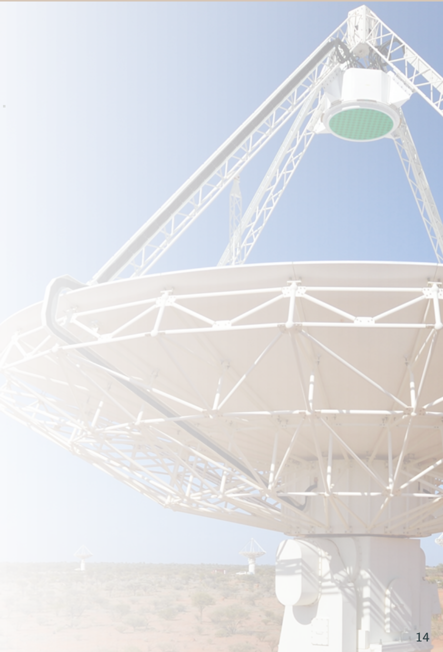

Some Systematic Effects

Some issues to consider:

- Catalogue completeness at some S_ν.
- Declination-dependent systematics.
- Contamination from the Galactic plane and bright radio sources.

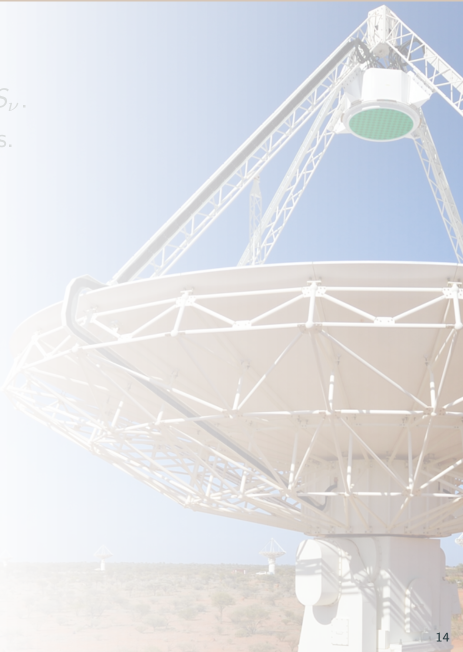

Some Systematic Effects

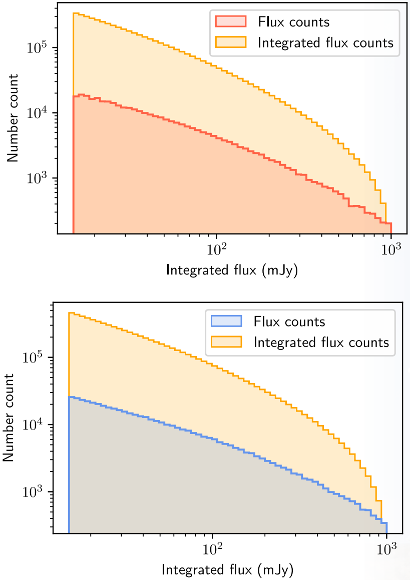

Figure 9: Flux density distribution for NVSS and RACS-low. $15\,\text{mJy} < S_{\text{int.}} < 1000\,\text{mJy}$.

Preparing NVSS & RACS

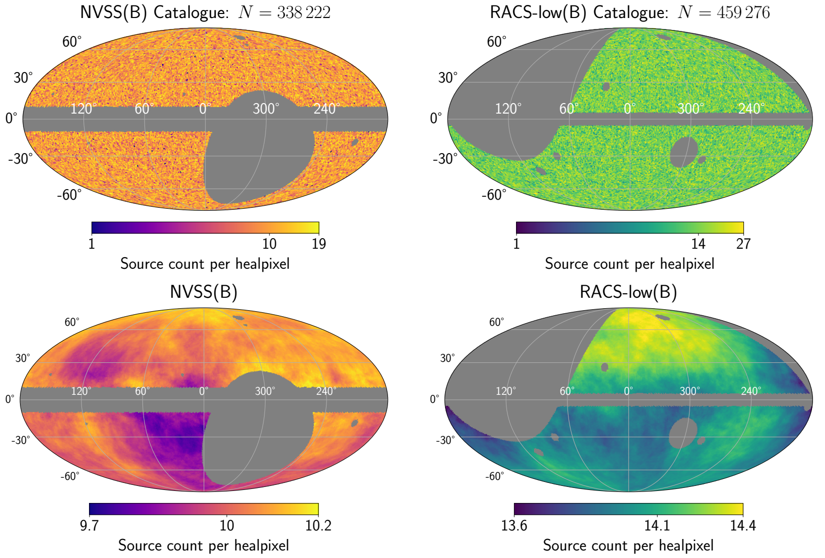

Figure 10: NVSS and RACS-low samples in Galactic coordinates binned into healpixels. *Top:* Raw density maps. *Bottom:* Smoothed density maps.

Cross-matching Local Sources

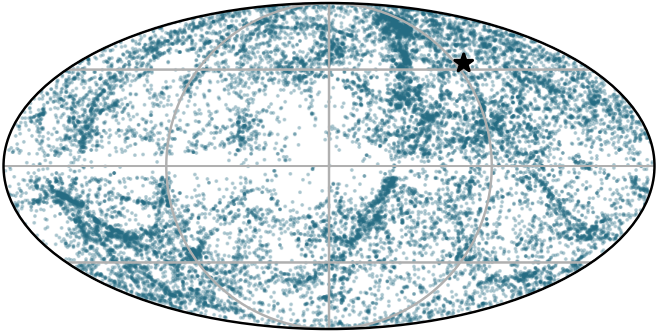

Remove **nearby structure**, which complicates the picture.

Cross-match NVSS and RACS-low radio sources with counterparts:
2MRS (near-IR); **NED** (radio).

Cross-matching Local Sources

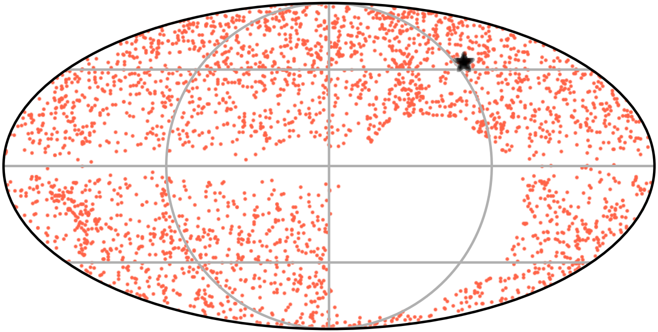

Remove **nearby structure**, which complicates the picture.

Cross-match NVSS and RACS-low radio sources with counterparts: **2MRS** (near-IR); **NED** (radio).

Cross-matching Local Sources

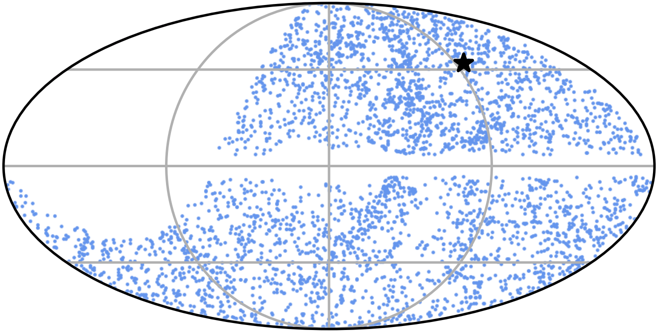

Remove **nearby structure**, which complicates the picture.

Cross-match NVSS and RACS-low radio sources with counterparts:
2MRS (near-IR); **NED** (radio).

Statistics: Bayesian Inference

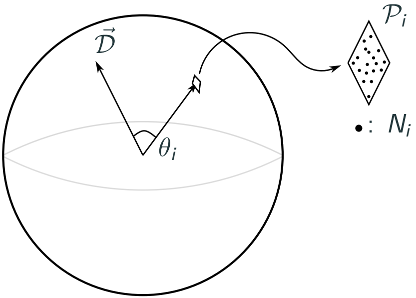

Figure 11: Schematic of pixel $\mathcal{P}_i$ on the celestial sphere with N_i sources $(\cdot)$ near dipole vector $\vec{\mathcal{D}}$.

Dipole vector $\vec{\mathcal{D}}$ is a free parameter.

Statistics: Bayesian Inference

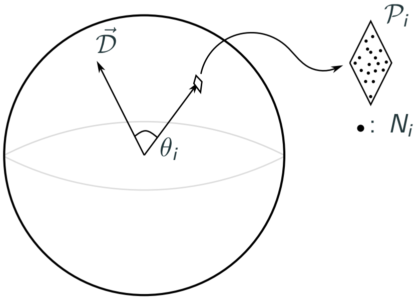

Figure 11: Schematic of pixel $\mathcal{P}_i$ on the celestial sphere with N_i sources $(\cdot)$ near dipole vector $\vec{\mathcal{D}}$.

Dipole vector $\vec{\mathcal{D}}$ is a free parameter.

- Pixel $\mathcal{P}_i$ has N_i sources.

Statistics: Bayesian Inference

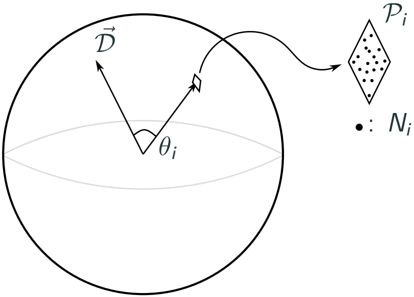

Figure 11: Schematic of pixel $\mathcal{P}_i$ on the celestial sphere with N_i sources $(\cdot)$ near dipole vector $\vec{\mathcal{D}}$.

Dipole vector $\vec{\mathcal{D}}$ is a free parameter.

- Pixel $\mathcal{P}_i$ has N_i sources.
- $\mathbb{E}[N_i] = \bar{N}(1 + \mathcal{D}\cos\theta_i)$

Statistics: Bayesian Inference

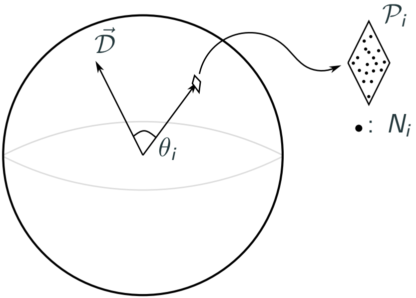

Figure 11: Schematic of pixel $\mathcal{P}_i$ on the celestial sphere with N_i sources $(\cdot)$ near dipole vector $\vec{\mathcal{D}}$.

Dipole vector $\vec{\mathcal{D}}$ is a free parameter.

- Pixel $\mathcal{P}_i$ has N_i sources.
- $\mathbb{E}[N_i] = \bar{N}(1 + \mathcal{D}\cos\theta_i)$
- Construct a probability map over the sky.

Statistics: Bayesian Inference

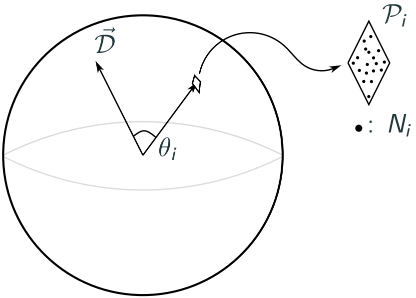

Figure 11: Schematic of pixel $\mathcal{P}_i$ on the celestial sphere with N_i sources ($\cdot$) near dipole vector $\vec{\mathcal{D}}$.

Dipole vector $\vec{\mathcal{D}}$ is a free parameter.

- Pixel $\mathcal{P}_i$ has N_i sources.
- $\mathbb{E}[N_i] = \bar{N}(1 + \mathcal{D}\cos\theta_i)$
- Construct a probability map over the sky.

Yields a likelihood function $\mathcal{L}$ which we can plug into Bayes' theorem

$$P(\Theta|\mathbf{D}, M) = \frac{\mathcal{L}(\mathbf{D}|\Theta, M)\pi(\Theta|M)}{\mathcal{Z}(\mathbf{D}|M)}.$$

Statistics: Bayesian Inference

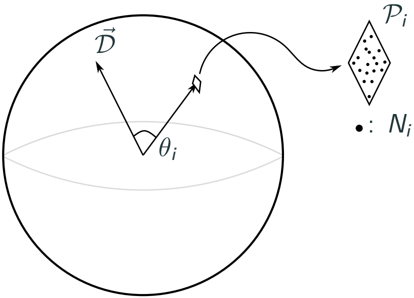

Figure 11: Schematic of pixel $\mathcal{P}_i$ on the celestial sphere with N_i sources $(\cdot)$ near dipole vector $\vec{\mathcal{D}}$.

Dipole vector $\vec{\mathcal{D}}$ is a free parameter.

- Pixel $\mathcal{P}_i$ has N_i sources.
- $\mathbb{E}[N_i] = \bar{N}(1 + \mathcal{D}\cos\theta_i)$
- Construct a probability map over the sky.

Yields a likelihood function $\mathcal{L}$ which we can plug into Bayes' theorem

$$P(\Theta|\mathbf{D}, M) = \frac{\mathcal{L}(\mathbf{D}|\Theta, M)\pi(\Theta|M)}{\mathcal{Z}(\mathbf{D}|M)}.$$

Use a Bayesian statistical approach to infer posterior probability distribution for $\Theta = \{\mathcal{D}, l, b\}$. Analyse individually and jointly.

Likelihood Function

How do we write down our likelihood function?

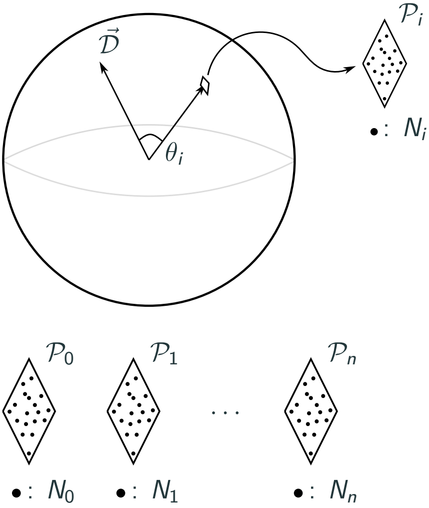

Likelihood Function

How do we write down our likelihood function?

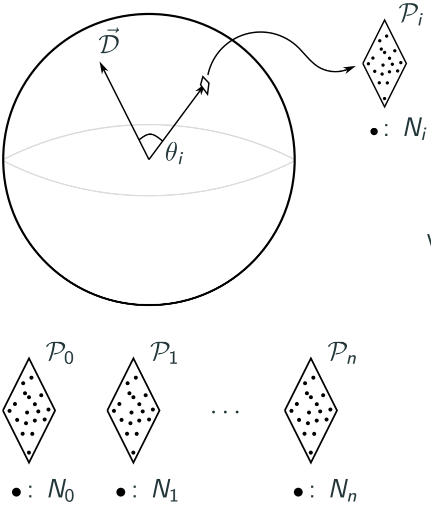

$$P(N_i|\lambda_i) = \text{Pois}(\lambda_i)$$

where $\lambda_i = \bar{N}(1 + \mathcal{D}\cos\theta_i)$. So,

$$\ln \mathcal{L} = \sum_{i=0}^{n} \ln\left[\text{Pois}(N_i|\lambda_i)\right].$$

Likelihood Function

How do we write down our likelihood function?

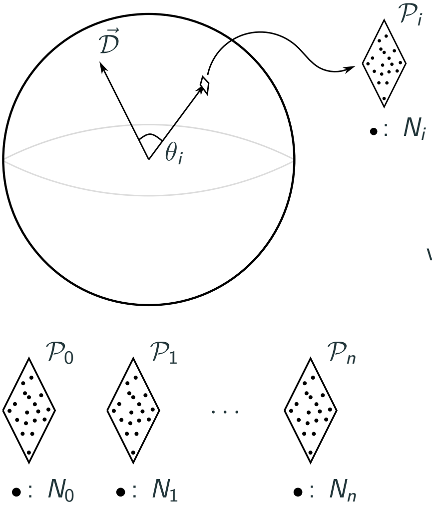

$$\hat{f}(\widehat{\mathbf{p}}_i) = \frac{f(\widehat{\mathbf{p}}_i)}{\sum_{i=0}^{n} f(\widehat{\mathbf{p}}_i)}$$

where $f_i = 1 + \mathcal{D}\cos\theta_i$. So,

$$\ln \mathcal{L} = \sum_{i=0}^{n} N_i \ln \hat{f}(\widehat{\mathbf{p}}_i)$$

Model Comparison

	Short label	Description
M_0	Null	Monopole
M_1	Free dipole	Free $\mathcal{D}$, l, b
M_2	Kinematic velocity	$\mathcal{D}$ fixed and free l, b
M_3	Kinematic direction	l, b fixed and free $\mathcal{D}$
M_4	Kinematic dipole	All parameters fixed to CMB expectation
M_5	W23	$\mathcal{D}$, l, b from Wagenveld et al. (2023)

Table 1: The six models tested and ranked.

Compare models' explanatory power with marginal likelihood $\mathcal{Z}(\mathbf{D}|M)$.

This gives us the Bayes factor $\ln B_{i0} = \ln \mathcal{Z}_i - \ln \mathcal{Z}_0$.

Results

NVSS & RACS: Individual Results

$$\boxed{\mathcal{D}_{\mathsf{CMB}} \approx 0.004}$$

NVSS & RACS: Individual Results

$\mathcal{D}_{\mathrm{CMB}} \approx 0.004$

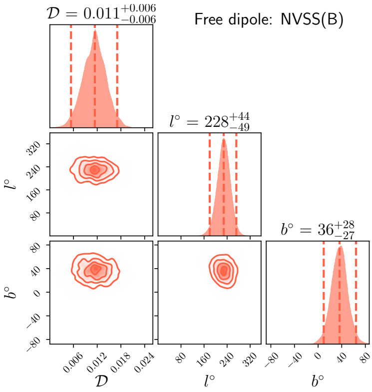

Model		$\ln B_{i0}$
M_1	Free dipole	3.1
M_3	Kin. direction	4.5
M_4	Kin. dipole	4.8

NVSS & RACS: Individual Results

$\mathcal{D}_{\text{CMB}} \approx 0.004$

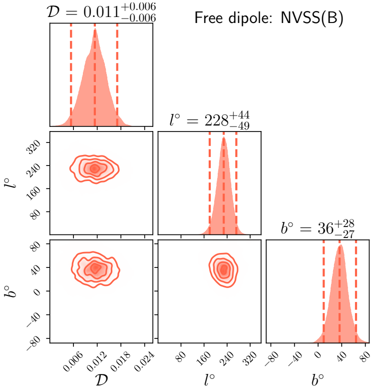

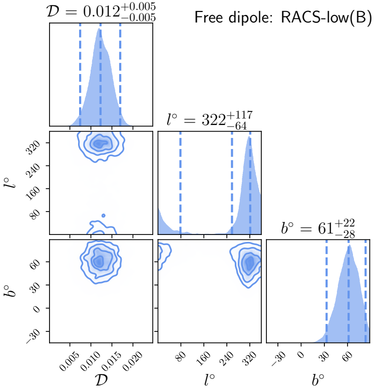

Model		$\ln B_{i0}$
M_1	Free dipole	3.1
M_3	Kin. direction	4.5
M_4	Kin. dipole	4.8

Model		$\ln B_{i0}$
M_1	Free dipole	8.2
M_3	Kin. direction	7.5
M_4	Kin. dipole	6.6

NVSS & RACS: Individual Results

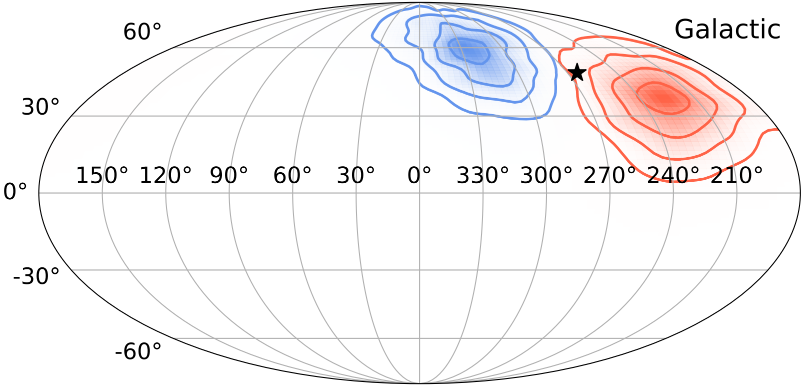

Figure 12: Projection of distribution for *l* and *b* onto the sky (Galactic coordinates) for RACS-low and NVSS. ★: CMB dipole.

$$\mathcal{D}_{\text{NVSS}} \approx (11 \pm 6) \times 10^{-3} \qquad \mathcal{D}_{\text{RACS}} \approx (12 \pm 5) \times 10^{-3}$$

Joint Analysis: NVSS + RACS-low

$\boxed{\mathcal{D}_{\mathsf{CMB}} \approx 0.004}$ — $\ln \mathcal{L} = \ln \mathcal{L}_{\mathsf{NVSS}} + \mathcal{L}_{\mathsf{RACS}}$

Joint Analysis: NVSS + RACS-low

$\boxed{\mathcal{D}_{\text{CMB}} \approx 0.004}$ — $\ln \mathcal{L} = \ln \mathcal{L}_{\text{NVSS}} + \mathcal{L}_{\text{RACS}}$

Free dipole: joint

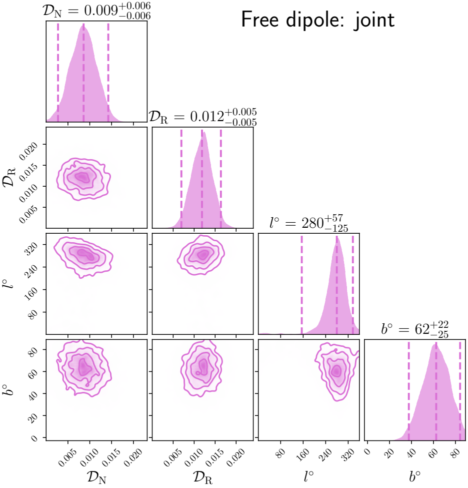

Joint Analysis: NVSS + RACS-low

$\boxed{\mathcal{D}_{\text{CMB}} \approx 0.004}$ — $\ln \mathcal{L} = \ln \mathcal{L}_{\text{NVSS}} + \mathcal{L}_{\text{RACS}}$

Free dipole: joint

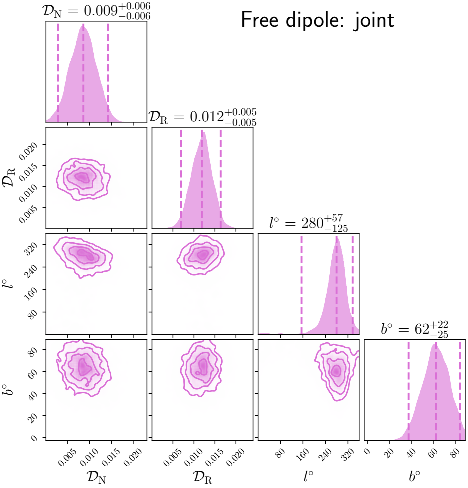

Model		$\ln B_{i0}$
M_3	Kin. dir.	12.1
M_4	Kin. dipole	11.4
M_5	W23	17.1

M_3 (kinematic direction):

$\mathcal{D}_{\text{NVSS}} \approx (10 \pm 5) \times 10^{-3}$

$\mathcal{D}_{\text{RACS}} \approx (11 \pm 5) \times 10^{-3}$

Joint Analysis: Dipole Position Distribution

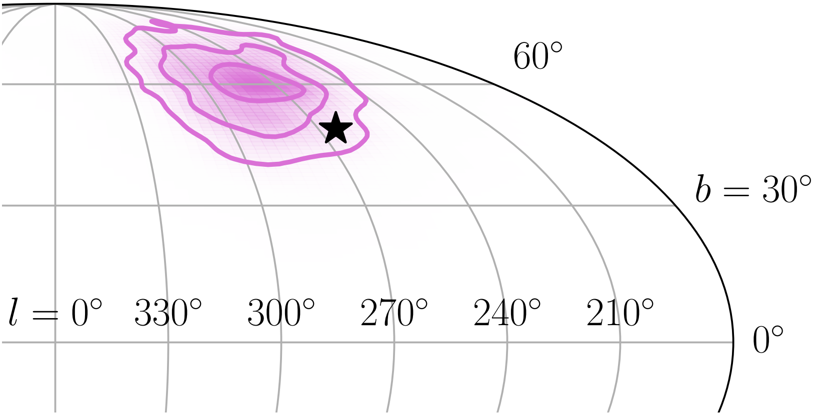

Figure 13: Projection of marginal distribution for *l* and *b* onto the sky, Galactic coordinates. ★: CMB dipole.

The Effect of Local Clustering

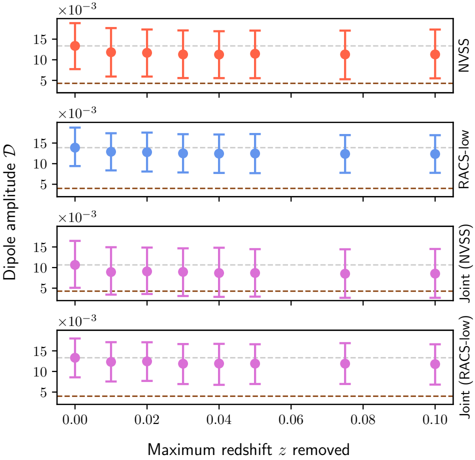

Figure 14: Inferred dipole amplitude by redshift of local source removed.

As sources up to $z \approx 0.03$ ($\approx 130\,\mathrm{Mpc}$) are removed, the inferred dipole amplitude decreases by 10%–15%.

Still not enough to explain the amplitude tension.

Clustering Dipole

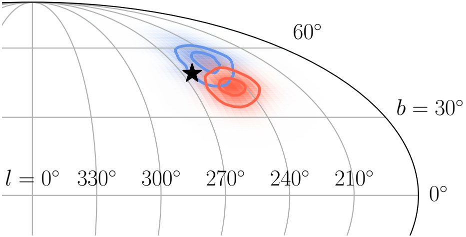

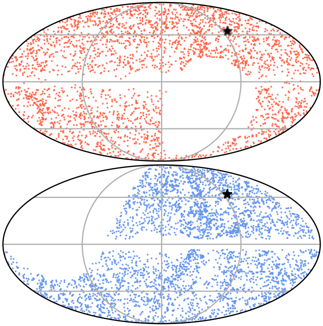

Figure 15: Inferred clustering dipole. *Star:* CMB dipole. *Red:* Dipole in cross-matched NVSS sources. *Blue:* Dipole in cross-matched RACS-low sources. *Both:* $\mathcal{D} \approx 0.25$.

The clustering dipole aligns with the CMB dipole!?

NVSS and RACS Amplitudes

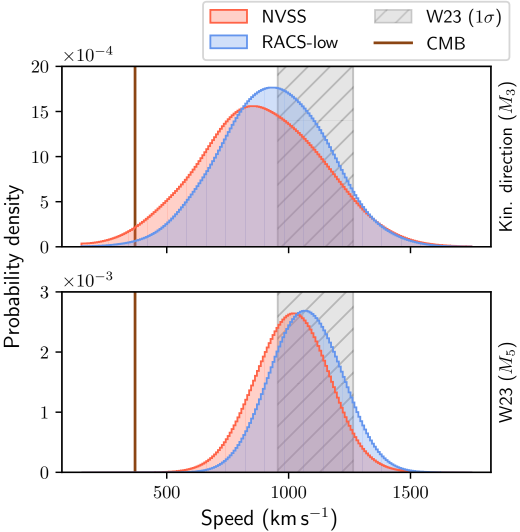

Figure 16: Marginal PDF for inferred heliocetric velocity. *Brown:* Expectation from CMB dipole. *Grey:* Results of Wagenveld et al. (2023). *Red/blue:* Our results.

The picture is somewhat similar — an amplitude ×2–3 larger than the CMB expectation is preferred.

Conclusions

Summary

$\mathcal{D}$ Measurements, Radio+IR+Optical

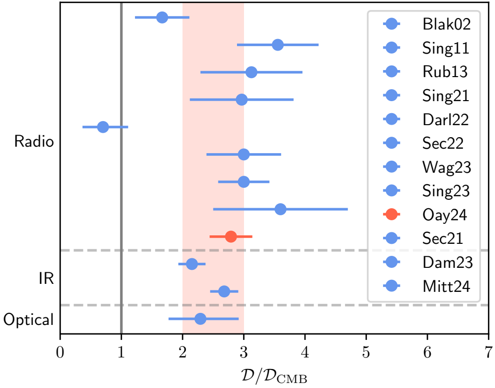

Figure 17: Literature values for $\mathcal{D}$ including results from our work (red) and other studies (blue).

There is a trend towards an excessive dipole (2 to $3 \times \mathcal{D}_{\rm CMB}$) across radio, optical and IR surveys.

Summary

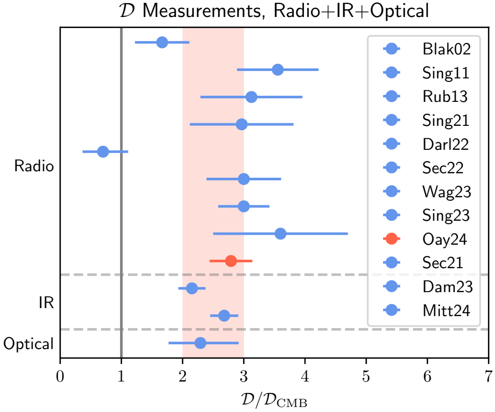

Figure 17: Literature values for $\mathcal{D}$ including results from our work (red) and other studies (blue).

There is a trend towards an excessive dipole (2 to $3 \times \mathcal{D}_{\mathrm{CMB}}$) across radio, optical and IR surveys.

This corresponds to $v \approx 1000\,\mathrm{km\,s^{-1}}$, not the $370\,\mathrm{km\,s^{-1}}$ we get from the CMB.

Summary

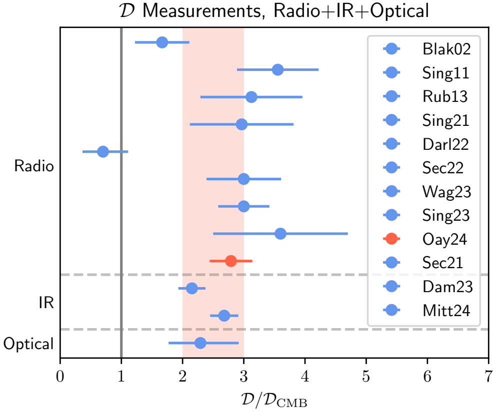

Figure 17: Literature values for $\mathcal{D}$ including results from our work (red) and other studies (blue).

There is a trend towards an excessive dipole (2 to $3 \times \mathcal{D}_{\mathrm{CMB}}$) across radio, optical and IR surveys.

This corresponds to $v \approx 1000\,\mathrm{km\,s^{-1}}$, not the $370\,\mathrm{km\,s^{-1}}$ we get from the CMB.

The Hubble H_0 tension is $\approx 10\%$. This dipole tension is 100%–200% and has reached 5σ in Secrest et al. (2021, 2022); Dam et al. (2023).

Outlook — RACS-mid

RACS-mid (1367.5 MHz) has been available as of last year. But there are some issues to understand first.

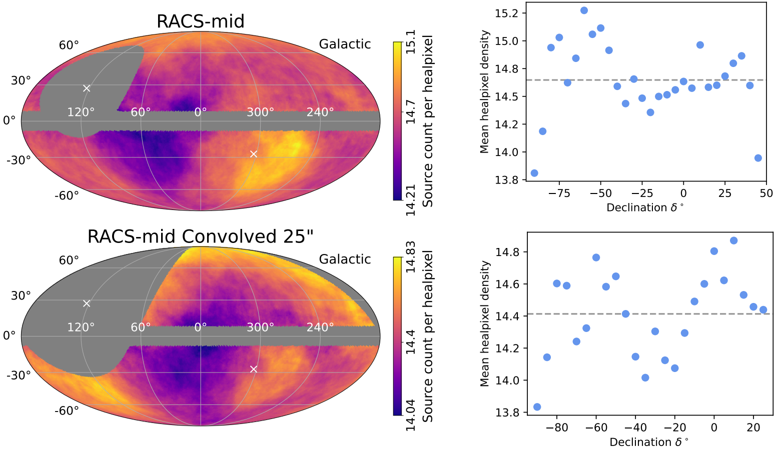

Figure 18: 10 mJy $< S_{\mathrm{int.}} <$ 1000 mJy. *Left:* smoothed RACS-mid maps (Galactic coordinates). *Right:* Mean density vs declination.

Outlook

- What can we do in the future?
- Radio — RACS-mid, RACS-high?
  - Need to understand systematics better
  - There are some declination-dependent effects in RACS-mid which persist in the convolved 25” catalogue
- Other dipoles? e.g. Type Ia SNe

arXiv

See the paper here!

2406.01871

What is going on? Is the cosmological principle wrong? Or are there other systematics?

References

Dam L., Lewis G. F., Brewer B. J., 2023, MNRAS, 525, 231

Ellis G. F. R., Baldwin J. E., 1984, MNRAS, 206, 377

Mittal V., Oayda O. T., Lewis G. F., 2024, MNRAS, 527, 8497

Planck Collaboration et al., 2020, A&A, 641, A4

Secrest N. J., von Hausegger S., Rameez M., Mohayaee R., Sarkar S., Colin J., 2021, ApJ, 908, L51

Secrest N. J., von Hausegger S., Rameez M., Mohayaee R., Sarkar S., 2022, ApJ, 937, L31

Wagenveld J. D., Klöckner H.-R., Schwarz D. J., 2023, A&A, 675, A72